

Time-dependent fluid squeeze-out between solids with rough surfaces

B. Lorenz^{1,2} and B.N.J. Persson^{1,a}

¹ IFF, FZ Jülich, D-52425 Jülich, Germany

² IFAS, RWTH Aachen University, D-52074 Aachen, Germany

Received 19 March 2010

Published online: 28 July 2010 – © EDP Sciences / Società Italiana di Fisica / Springer-Verlag 2010

Abstract. We study the time dependency of the (average) interfacial separation between an elastic solid with a flat surface and a rigid solid with a randomly rough surface, squeezed together in a fluid. As an application we discuss fluid squeeze-out between a tire tread block and a road surface. Some implications for the leakage of seals are discussed, and experimental results are presented to test the theory. The theoretical prediction for the leak rate as a function of the fluid pressure difference is in good agreement with the experimental data for all fluid pressures up to “lift-off”, where the fluid pressure equals the nominal rubber-substrate squeezing pressure.

1 Introduction

Contact mechanics between solid surfaces is the basis for understanding many tribology processes [1–7], such as friction, adhesion, wear and sealing. The two most important properties in contact mechanics are the area of real contact and the interfacial separation between the solid surfaces. For non-adhesive contact and small squeezing pressure, the average interfacial separation depends logarithmically on the squeezing pressure [8, 9], and the (projected) contact area depends linearly on the squeezing pressure [10]. Here we study how the (average) interfacial separation depends on time when two elastic solids with rough surfaces are squeezed together in a fluid. In particular, we calculate the time necessary to squeeze out the fluid from the contact regions between the solids. As an application we discuss fluid squeeze-out between a tire tread block and a road surface. Some implications for the leakage of seals are discussed, and experimental data are presented to test the theory.

2 Squeeze-out: large separation

Consider an elastic solid with a flat surface squeezed in a fluid against a rigid solid with a randomly rough surface, see fig. 1. The fluid is assumed to be Newtonian with viscosity η . The upper solid is a cylindrical block with radius R , elastic modulus E and Poisson ratio ν . The bottom surface of the cylinder is perfectly flat, and the substrate randomly rough with root-mean-square roughness

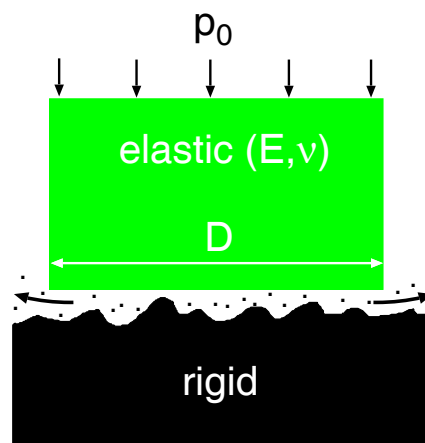


Fig. 1. The upper solid, a cylindrical block with diameter $D = 2R$, the elastic modulus E and the Poisson ratio ν , is squeezed in a fluid against a rigid substrate. The bottom surface of the cylinder is perfectly flat and the substrate surface randomly rough with the root-mean-square roughness amplitude h_{rms} .

amplitude h_{rms} . Here we focus first on the simplest possible situation which can be studied analytically, where the (macroscopic or locally averaged) pressure distribution in the fluid gives rise to negligible deformations of the bottom surface of the elastic block. This requires that the amplitude δu of the (fluid-induced) elastic deformations is much smaller than h_{rms} . Since δu is typically of order (or smaller than) $\approx p_0 R / E^*$, where $E^* = E / (1 - \nu^2)$ and p_0 the pressure applied to the upper surface of the

^a e-mail: b.persson@fz-juelich.de

cylinder block, we get the condition $h_{\text{rms}} \gg p_0 R/E^*$. For elastically stiff materials with $E^* \approx 10^{11}$ Pa and for $R = 1$ cm we get $p_0 R/E^* < 0.1 \mu\text{m}$ if $p_0 < 1$ MPa. For tread rubber $E^* \approx 10$ MPa and if $p_0 \approx 0.3$ MPa we get $p_0 R/E^* \approx 0.3$ mm which is smaller than the root-mean-square roughness of many asphalt road surfaces. In many applications a thin rubber film, coating a hard solid, is in contact with an elastically hard countersurface. If the linear size of the contact region is large compared to the rubber film thickness, this geometry will strongly suppress the (fluid-induced) deformations of the rubber film on the length scale of the linear size of the nominal contact area, and most of the (non-uniform) deformations of the rubber film is due to the interaction with the substrate asperities.

We first develop a theory which should be accurate for large enough interfacial separation, *e.g.*, corresponding to the early phase of the squeeze-out process. We assume that the longest wavelength roughness component, λ_0 , is small compared to the linear size R of the (apparent) contact region. In this case we can speak about locally averaged (over surface areas with linear dimension of order λ_0) quantities.

Neglecting inertia effects, the squeeze-out is determined by (see, *e.g.*, ref. [5])

$$\frac{d\bar{u}}{dt} \approx -\frac{2\bar{u}^3 \bar{p}_{\text{fluid}}(t)}{3\eta R^2}, \quad (1)$$

where $\bar{p}_{\text{fluid}}(t)$ is the (average) fluid pressure, and \bar{u} the (locally averaged) interfacial separation. If p_0 is the applied pressure acting on the top surface of the cylinder block, we have

$$\bar{p}_{\text{fluid}}(t) = p_0 - p_{\text{cont}}(t), \quad (2)$$

where p_{cont} is the asperity contact pressure. We will first assume that the pressure p_0 is so small that for all times $u \gg h_{\text{rms}}$. In this case we can use the asymptotic relation [8]

$$p_{\text{cont}} \approx \beta E^* \exp\left(-\frac{\bar{u}}{u_0}\right), \quad (3)$$

where $u_0 = h_{\text{rms}}/\alpha$. The parameters α and β depend on the fractal properties of the rough surface [8].

From (3) we get

$$\frac{d\bar{u}}{dt} \approx -\frac{u_0}{p_{\text{cont}}} \frac{dp_{\text{cont}}}{dt}. \quad (4)$$

Using (4) and (2) we get from (1)

$$\frac{dp_{\text{cont}}}{dt} \approx \frac{2\bar{u}^3(p_{\text{cont}}(t))}{3\eta R^2 u_0} p_{\text{cont}}(p_0 - p_{\text{cont}}). \quad (5)$$

For long times $p_{\text{cont}} \approx p_0$ and we can approximate (5) with

$$\frac{dp_{\text{cont}}}{dt} \approx \frac{2\bar{u}^3(p_0)}{3\eta R^2 u_0} p_0(p_0 - p_{\text{cont}}).$$

Integrating this equation gives

$$p_{\text{cont}}(t) \approx p_0 - [p_0 - p_{\text{cont}}(0)] \exp\left(-\left(\frac{\bar{u}(p_0)}{h_{\text{rms}}}\right)^3 \frac{t}{\tau}\right),$$

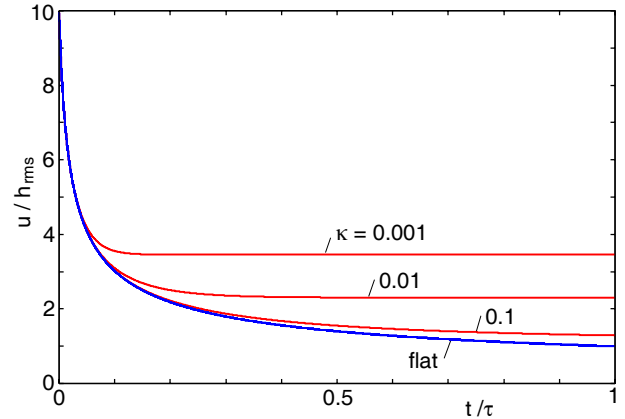


Fig. 2. (Colour on-line) The interfacial separation (or film thickness) \bar{u} (in units of h_{rms}) as a function of the squeeze time t (in units of τ) for several values of the parameter κ . For each squeeze pressure, the upper (red) lines are the result for the rough surfaces while the lower (blue) line is for flat surfaces.

where

$$\tau = \frac{3\eta R^2 u_0}{2h_{\text{rms}}^3 p_0} = \frac{3\eta R^2}{2\alpha h_{\text{rms}}^2 p_0}. \quad (6)$$

Using (3) this gives

$$\bar{u} \approx u_\infty + \left(1 - \frac{p_{\text{cont}}(0)}{p_0}\right) u_0 \exp\left(-\left(\frac{\bar{u}(p_0)}{h_{\text{rms}}}\right)^3 \frac{t}{\tau}\right),$$

where $u_\infty = u_0 \log(\beta E^*/p_0)$. Thus, $\bar{u}(t)$ will approach the equilibrium separation u_∞ in an exponential way, and we can define the squeeze-out time as the time to reach, say, $1.01u_\infty$. For flat surfaces, within continuum mechanics, the film thickness approaches zero as $t \rightarrow \infty$ as $\bar{u} \sim t^{-1/2}$. Thus in this case it is not possible to define a meaningful fluid squeeze-out time.

Let us measure distance \bar{u} in units of h_{rms} , pressure in units of p_0 and time in units of τ (eq. (6)). In these units (5) takes the form

$$\frac{dp_{\text{cont}}}{dt} \approx \bar{u}^3 p_{\text{cont}}(1 - p_{\text{cont}}). \quad (7)$$

In the same units (3) takes the form

$$p_{\text{cont}} \approx \kappa^{-1} \exp(-\alpha \bar{u}), \quad (8)$$

where

$$\kappa = \frac{p_0}{\beta E^*}. \quad (9)$$

In fig. 2 we show the interfacial separation (or film thickness) \bar{u} (in units of h_{rms}) as a function of the squeeze time t (in units of τ) for several values of the parameter κ . For each κ value, the upper (red) lines are the result for the rough surfaces while the lower (blue) lines are for flat surfaces. In the calculation we have used $\alpha = 0.5$ and $\beta = 1$.

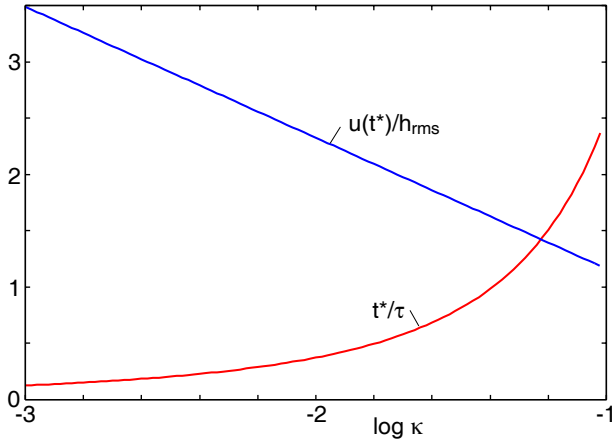


Fig. 3. The fluid squeeze-out time t^* (in units of τ) and the final interfacial separation (or film thickness), $\bar{u}(t^*)$ (in units of h_{rms}), as a function of the logarithm (with 10 as basis) of the parameter κ . We define t^* so that $\bar{u}(t^*) = 1.01\bar{u}(\infty)$.

In fig. 3 we show the fluid squeeze-out time t^* (in units of τ) and the final interfacial separation (or film thickness), $\bar{u}(t^*)$ (in units of h_{rms}), as a function of the parameter κ . We define t^* so that $\bar{u}(t^*) = 1.01\bar{u}(\infty)$.

At high enough squeezing pressures, the interfacial separation after long enough times will be smaller than h_{rms} , and the asymptotic relation (3) will no longer hold. In this case the relation $p_{\text{cont}}(\bar{u})$ can be calculated using the equations given in ref. [1] (see also appendix A). Substituting (2) in (1) and measuring pressure in units of p_0 , separation in units of h_{rms} and time in units of τ , one obtains

$$\frac{d\bar{u}}{dt} \approx -\alpha^{-1}\bar{u}^3(1 - p_{\text{cont}}), \quad (10)$$

where $\alpha = h_{\text{rms}}/u_0$. This equation together with the relation $p_{\text{cont}}(\bar{u})$ constitute two equations for two unknown (\bar{u} and p_{cont}) which are easily solved by numerical integration. In what follows we refer to the theory presented above as the average-separation theory.

3 Squeeze-out: general theory

We now present a general theory of squeeze-out, which is accurate for small separation and which reduces to the result presented in sect. 2 for large separation. The theory presented below is based on a recently developed theory of the leak rate of (static) seals [11]. We assume again that the longest wavelength roughness component, λ_0 , is small compared to the linear size R of the (apparent) contact region. In this case we can speak about locally averaged (over surface areas with linear dimension of order λ_0) quantities. Let $\mathbf{J}(\mathbf{x}, t)$ be the (locally averaged) 2D-fluid flow vector which satisfies the continuity equation

$$\nabla \cdot \mathbf{J} + \frac{\partial \bar{u}}{\partial t} = 0, \quad (11)$$

where $\bar{u}(\mathbf{x}, t)$ is the (locally averaged) surface separation or, equivalently, the 2D-fluid density (fluid volume per

unit area). Here and in what follows

$$\mathbf{J} = (J_x, J_y), \quad \nabla = (\partial_x, \partial_y) \quad (12)$$

are 2D vectors. In ref. [11] we have shown that within an effective medium approach

$$\mathbf{J} = -\sigma_{\text{eff}} \nabla p_{\text{fluid}}, \quad (13)$$

where $p_{\text{fluid}}(\mathbf{x}, t)$ is the (locally averaged) fluid pressure and where the effective conductivity $\sigma_{\text{eff}}(p_{\text{cont}})$ depends on the (locally averaged) contact pressure $p_{\text{cont}}(\mathbf{x}, t)$. (Note that σ_{eff} is proportional to the so-called pressure flow factor [12–14].) Note that when inertia effects are negligible

$$\int d^2x [p_{\text{cont}}(\mathbf{x}, t) + p_{\text{fluid}}(\mathbf{x}, t)] = F_N(t) \quad (14)$$

is the applied normal load. The function $\sigma_{\text{eff}}(p_{\text{cont}})$ can be calculated from the surface roughness power spectrum and the (effective) elastic modulus as described in ref. [11]. Substituting (13) in (11) gives

$$\nabla \cdot [\sigma_{\text{eff}} \nabla p_{\text{fluid}}] = \frac{\partial \bar{u}}{\partial t}. \quad (15)$$

Equation (15) together with the relation $p_{\text{cont}}(\bar{u})$ and the (standard) expression relating the macroscopic deformation $\bar{u}(\mathbf{x}, t)$ to the local pressure $p_0(\mathbf{x}) = p_{\text{cont}}(\mathbf{x}, t) + p_{\text{fluid}}(\mathbf{x}, t)$ constitutes three equations for the three unknown p_{cont} , p_{fluid} and \bar{u} . In addition one needs the effective medium expression for $\sigma_{\text{eff}}(p_{\text{cont}})$, and the “boundary condition” (14) must be satisfied. Here we will not study the most general problem but we focus on the limiting case discussed above where the macroscopic deformations of the solid walls can be neglected. In this case \bar{u} and p_{cont} will only depend on time. As a result $\sigma_{\text{eff}}(p_{\text{cont}})$ will only depend on time. Thus, (15) reduces to

$$\sigma_{\text{eff}} \nabla^2 p_{\text{fluid}} = \frac{d\bar{u}}{dt}. \quad (16)$$

Since the right-hand side only depends on time,

$$p_{\text{fluid}}(\mathbf{x}, t) = 2\bar{p}_{\text{fluid}}(t) [1 - (r/R)^2], \quad (17)$$

where $\bar{p}_{\text{fluid}}(t)$ is the average (nominal) fluid pressure in the nominal contact region. Substituting (17) in (16) gives

$$\frac{8\sigma_{\text{eff}}}{R^2} \bar{p}_{\text{fluid}} = -\frac{d\bar{u}}{dt}. \quad (18)$$

Equation (14) takes the form

$$p_{\text{cont}} + \bar{p}_{\text{fluid}} = p_0. \quad (19)$$

Using (4) and (19) in (18) gives

$$\frac{dp_{\text{con}}}{dt} \approx \frac{8\sigma_{\text{eff}}(p_{\text{cont}})}{R^2 u_0} p_{\text{cont}}(p_0 - p_{\text{cont}}). \quad (20)$$

From this equation one obtains $p_{\text{cont}}(t)$, and using (3) and (19) one can then calculate $\bar{u}(t)$ and $p_{\text{fluid}}(t)$. As

shown in appendix A, when $p_{\text{cont}} \rightarrow 0$, $\bar{u} \rightarrow \infty$ and $\sigma_{\text{eff}} \rightarrow \bar{u}^3/12\eta$, which is an exact result to zero order in h_{rms}/\bar{u} . Substituting $\sigma_{\text{eff}} = \bar{u}^3/12\eta$ in (20) gives (5). Thus, in the limit of small pressures p_0 , the present treatment reduces to the average-separation theory of sect. 2, which is exact when the average separation \bar{u} between the surfaces is large (which is the case for all times if the pressures p_0 is small). We will refer to $\sigma_{\text{eff}} = \bar{u}^3/12\eta$ as the average-separation expression for σ_{eff} .

Let us study the squeeze-out for long times. For long times $p_{\text{cont}} \approx p_0$ and we can approximate (20) with

$$\frac{dp_{\text{cont}}}{dt} \approx \frac{8\sigma_{\text{eff}}(p_0)}{R^2 u_0} p_0 (p_0 - p_{\text{cont}}). \quad (21)$$

Integrating this equation gives

$$p_{\text{cont}}(t) \approx p_0 - [p_0 - p_{\text{cont}}(0)] \exp\left(-\frac{8\sigma_{\text{eff}}(p_0)p_0}{R^2 u_0} t\right),$$

so that $p_{\text{cont}}(t)$ approaches p_0 (and $\bar{u}(t)$ approaches u_∞) in an exponential way, just as for the simpler model studied in sect. 2.

If we measure pressure in units of p_0 , separation \bar{u} in units of h_{rms} , and time in units of τ , eq. (20) takes the form

$$\frac{dp_{\text{cont}}}{dt} = \bar{\sigma}_{\text{eff}} p_{\text{cont}} (1 - p_{\text{cont}}), \quad (22)$$

where

$$\bar{\sigma}_{\text{eff}} = 12\eta\sigma_{\text{eff}}/h_{\text{rms}}^3. \quad (23)$$

The relation between p_{cont} and \bar{u} is given by (3).

At high enough squeezing pressures, the interfacial separation after long enough times will be smaller than h_{rms} , and the asymptotic relation (3) no longer holds. In this case the relation $p_{\text{cont}}(\bar{u})$ can be calculated using the equations given in ref. [1] (see also appendix A). Substituting (19) in (18) and measuring pressure in units of p_0 , separation in units of h_{rms} and time in units of τ , one obtains

$$\frac{d\bar{u}}{dt} = -\alpha^{-1} \bar{\sigma}_{\text{eff}} (1 - p_{\text{cont}}). \quad (24)$$

This equation, together with the relations $p_{\text{cont}}(\bar{u})$ and $\sigma_{\text{eff}}(p_{\text{cont}})$, constitute three equations for three unknown (\bar{u} , p_{cont} and σ_{eff}) which are easily solved by numerical integration. In the critical-junction theory which we will use below $\sigma_{\text{eff}} = (\alpha' u_1(\zeta_c))^3/12\eta$, where the separation $u_1(\zeta_c)$ is defined in ref. [11] (see also appendix A) and where $\alpha' < 1$ is a number of order unity (see ref. [11] where α' is denoted by α).

Figure 4 shows the calculated interfacial separation $\bar{u}(t)$ as a function of the squeeze time t for a silicon rubber block (elastic modulus $E = 2.3$ MPa) squeezed against a rough copper surface (log-log scale with 10 as basis), with the power spectrum given in ref. [15]. Curves 1 and 2 are the theory predictions using (10) and (24), respectively. In (24) we have used σ_{eff} as calculated using the critical-junction theory described in ref. [11], which gives nearly the same result as the effective medium theory described in the same reference. Results are also shown for

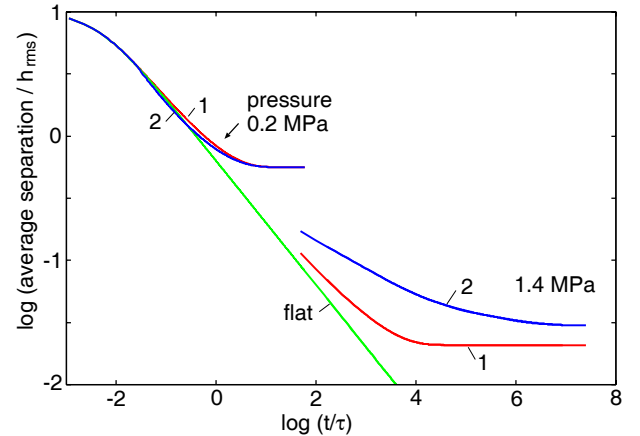


Fig. 4. The interfacial separation $\bar{u}(t)$ as a function of the squeeze time t for rough copper surface (log-log scale with 10 as basis). Curves 1 and 2 are the predictions using the average-separation theory and using the critical-junction theory, respectively. Results are also shown for a flat surface. The rubber block is assumed to be cylindrical with radius $R = 1.5$ cm. For a copper surface with root-mean-square roughness 0.12 mm; squeezing pressure $p_0 = 0.2$ MPa (upper curves) and 1.4 MPa. The elastic modulus $E = 2.3$ MPa.

a flat substrate surface. The rubber block is assumed to be cylindrical with the radius $R = 1.5$ cm and the surface of the copper block has a root-mean-square roughness of 0.12 mm. The squeezing pressure $p_0 = 0.2$ MPa (upper curves) and 1.4 MPa (lower curves), corresponding to $\kappa = p_0/\beta E^* \approx 1.5$ and 10.3, respectively. Note that for the pressure $p_0 = 1.4$ MPa, after long enough time the area of real contact (at the highest magnification ζ_1), A , percolates (*i.e.*, $A/A_0 > 0.5$, see ref. [11]), and there is no fluid leak channel at the interface [16]. As a result, when the contact area percolates, the fluid is confined at the interface and is not able to leak out. Thus, even after a very long time the interfacial separation is larger than would be expected in the absence of trapped or confined fluid (*e.g.*, for dry contact), where no part of the load would be carried by the fluid.

Figure 5 shows the normalized contact pressure $p_{\text{con}}(t)/p_0$ as a function of the logarithm of the squeeze time t for the same system as in fig. 4. Curves 1 and 2 are the predictions using (10) and (24), respectively. Note that for the pressure $p_0 = 1.4$ MPa, even after a very long time $p_{\text{con}} < 0.9p_0$. This is again a consequence of the fact that the non-contact area does not percolate and the fluid is confined at the interface, and even after a very long time, more than 10% of the external load is carried by the confined fluid.

Following ref. [17] the analysis presented above may be extended to include the fluid-pressure-induced elastic deformation of the solid surfaces at the interface. It is also easy to include the dependency of the fluid viscosity on the local pressure or local surface separation. The former is important for elastically hard solids (high pressures), *e.g.*, steel, and the latter “confinement effect” even for elastically soft solids (low pressures) when the fluid film

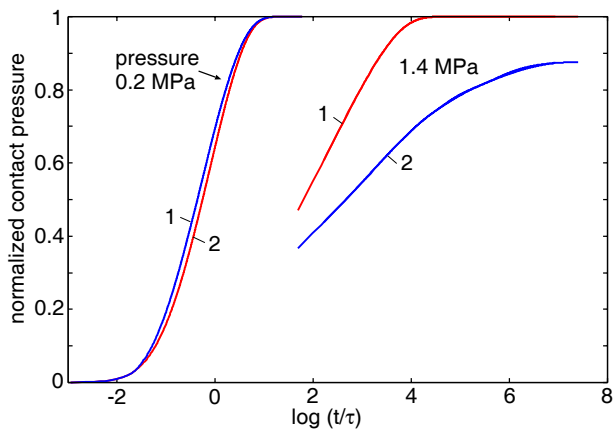


Fig. 5. The normalized contact pressure $p_{\text{con}}(t)/p_0$ as a function of the logarithm (with 10 as basis) of the squeeze time t for rough copper surface. Curves 1 and 2 are the predictions using the average-separation and using the critical-junction theory, respectively. The rubber block is assumed to be cylindrical with radius $R = 1.5$ cm. For a copper surface with root-mean-square roughness 0.12 mm; squeezing pressure $p_0 = 0.2$ MPa (upper curves) and 1.4 MPa. The elastic modulus $E = 2.3$ MPa.

thickness becomes of the order of a few nanometers or less [18].

Finally, let us note the following: The interfacial separation is usually mainly determined by the longest-wavelength surface roughness, which is observed close to the lowest magnification $\zeta \approx 1$; the shortest-wavelength (small amplitude) roughness has almost no influence on \bar{u} . However, it is also of great interest, *e.g.*, in the context of tire friction on wet road surface (see sect. 5), to study how the fluid is squeezed out from the (apparent) asperity contact regions observed at higher magnification ζ , see fig. 6. The theory developed above can be applied to this case too. Thus, let us study the squeeze-out of fluid from the apparent asperity contact regions observed at magnification ζ . At this magnification no surface roughness with wavelength below L/ζ can be observed. However, when the magnification is increased one observes shorter-wavelength roughness which will influence the fluid squeeze-out, and which may even result in sealed-off, trapped fluid. We can apply the theory above to study the squeeze-out of fluid from the asperity contact regions observed at magnification ζ by using, instead of the external pressure p_0 , the local squeezing pressure $p(\zeta) = p_0 A_0/A(\zeta)$, where $A(\zeta)$ is the (apparent) contact area observed at magnification ζ . The surface roughness in the contact regions is given by the surface power spectrum $C(q)$ for $q > \zeta/L$. With these modifications we can use the theory above to calculate the squeeze-out of fluid from the apparent asperity contact regions observed at the magnification ζ . One complication is, however, that the fluid is squeezed out from an asperity contact region into the surrounding, and the fluid pressure in the surrounding may be higher than the external pressure (which we have taken as our reference pressure in the study above) existing outside the nominal contact region observed at the

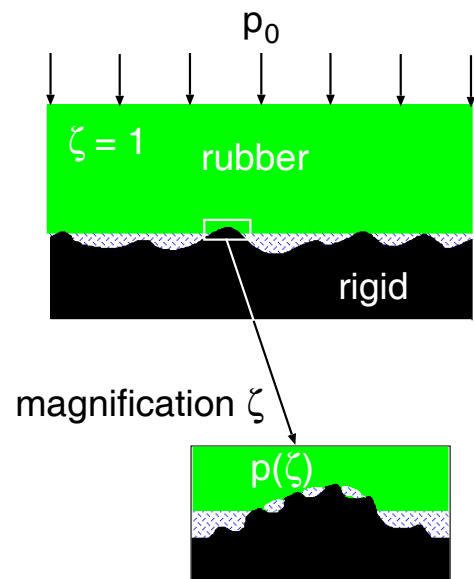


Fig. 6. A rubber block squeezed against a randomly rough substrate in a fluid. The (average) interfacial separation $\bar{u}(t)$ decreases with time t due to squeeze-out of the fluid. The time dependence of \bar{u} depends mainly on the long-wavelength roughness components. Nevertheless, the short-wavelength roughness components will affect the squeeze-out in asperity contact regions (observed at magnification ζ), which is relevant for, *e.g.*, rubber friction. This can be studied using the same theory applied to an asperity contact region by replacing the external pressure p_0 with the local squeezing pressure $p(\zeta)$ at the asperity (see text for details).

lowest magnification $\zeta = 1$. As a result, in order to study the squeeze-out from the asperity contact regions observed at magnification ζ' , one must first study the squeeze-out from the asperity contact regions observed at lower magnification $1 < \zeta < \zeta'$. We will not develop this theory here, but we believe a similar approach as that used to describe mixed lubrication for flat on flat in ref. [17] may be applied to the present problem.

4 Application to tire on wet road

As an application, consider a tire tread block squeezed against asphalt road surfaces in water. In figs. 7 and 8 we show the time dependence of the interfacial separation \bar{u} , and the difference $\Delta u = \bar{u}(t) - \bar{u}(\infty)$, respectively. In the calculation we have used the theory of sect. 2, which is valid in the present case where (for all times) $\bar{u} > 2h_{\text{rms}}$ (see below). We show results for two road surfaces, with the root-mean-square roughness 0.72 mm (surface 1) and 0.24 mm (surface 2). We assumed the squeezing pressure $p_0 = 0.2$ MPa and the elastic modulus $E = 10$ MPa. In the calculation we have used the surface roughness power spectrum obtained from the measured surface topographies. Note that for the smoother surface the squeeze-out time is roughly one decade longer than for the rougher asphalt road surface. In order for the water to have a negligi-

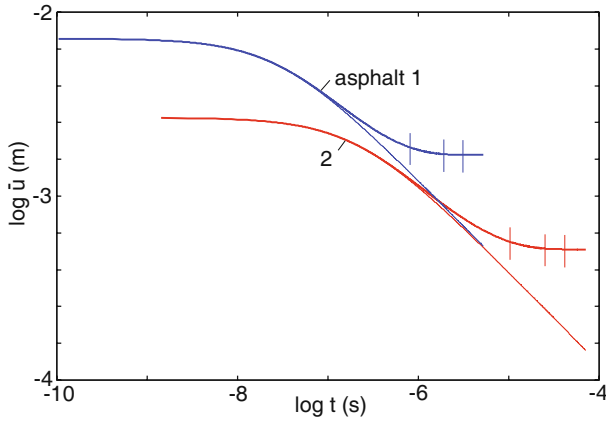


Fig. 7. The interfacial separation $\bar{u}(t)$ as a function of the squeeze time t for two asphalt road surfaces (log-log scale with 10 as basis). The tread block is assumed to be cylindrical with radius $R = 2$ cm. For two asphalt road surfaces with root-mean-square roughness 0.72 mm (surface 1) and 0.24 mm (surface 2). The nominal squeezing pressure $p_0 = 0.2$ MPa and the elastic modulus $E = 10$ MPa. The vertical lines denote (from left to right) the time when $\bar{u}(t)/\bar{u}(\infty) = 1.1, 1.01$ and 1.001 . The thin lines denote the fluid film thickness for perfectly flat surfaces. The calculations use the average-separation expression for σ_{eff} .

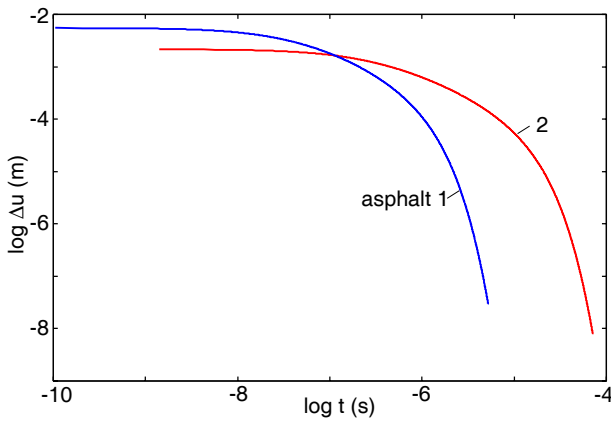


Fig. 8. The difference $\Delta u = \bar{u}(t) - \bar{u}(\infty)$ as a function of the squeeze time t for two asphalt road surfaces (log-log scale with 10 as basis). The tread block is assumed to be cylindrical with radius $R = 2$ cm. For two asphalt road surfaces with root-mean-square roughness 0.72 mm (surface 1) and 0.24 mm (surface 2). The squeezing pressure $p_0 = 0.2$ MPa and the elastic modulus $E = 10$ MPa.

ble influence on the hysteresis contribution to the friction, the water layer in the road-rubber contact regions must be smaller than $\sim 1 \mu\text{m}$. For the smoother road surface 2 it takes about $\sim 3 \times 10^{-5}$ s to reach $\Delta u = 1 \mu\text{m}$. If the tire rolling velocity is 30 m/s and the length of the tire footprint 0.1 m, then a tread block spends about 3×10^{-3} s in contact with the road. Thus, from the calculation above one may conclude that accounting just for the viscosity of the fluid (water) one expects (during rolling) almost complete fluid squeeze-out from the tread block road contact area, during most of the time the tread block spends

in the footprint. However, at the start of raining after a long time of dry road condition, the water will be mixed with contamination particles (*e.g.*, small rubber and road wear particles), and the effective viscosity of the mixture may be much larger than for pure water. In this case the squeeze-out may be incomplete, which could result in viscous hydroplaning during braking. In addition, even for pure water, regions of sealed off (trapped) fluid may appear at the interface, which will reduce the hysteresis contribution to the tire-road friction [19]. We note that during braking at small slip (below the maximum in the μ -slip curve) the tread block does not slip until close to the exit of the tire-road footprint, and the discussion above should therefore be valid for this case too.

It is interesting to compare the result above with the squeeze-out time due to inertia (but neglecting the viscosity). The time dependence of the squeeze-out for flat surfaces is given by (see ref. [20])

$$u(t) = u(0) \exp(-t/\tau'),$$

where

$$\tau' \approx \left(\frac{D^2 \rho}{64 p_0} \right)^{1/2}.$$

Thus, the time it takes to reduce the film thickness from $u(0)$ to a thickness of order h_{rms} is

$$t^* \approx \tau' \log[u(0)/h_{\text{rms}}].$$

If $u(0) = 1$ cm and $h_{\text{rms}} = 0.3$ mm, we get $t^* \approx \tau' \log(30) \approx 3.4\tau'$. With $D \approx 2$ cm, $p_0 \approx 0.3$ MPa and $\rho \approx 10^3$ kg/m³, we get $\tau' \approx 1.4 \times 10^{-4}$ s and $t^* \approx 5 \times 10^{-4}$ s.

5 Leakage of seals

In the calculation of the leak rate of seals presented in ref. [11] we neglected the influence of the fluid pressure on the contact mechanics. This is a good approximation as long as the squeezing pressure p_0 is much higher than the fluid pressure p_{fluid} , which was the case in the experiments presented in ref. [11]. However, in many practical situations it is not a good approximation to neglect the influence of the fluid pressure on the contact mechanics. Since the fluid pressure is higher on the fluid entrance side than on the fluid exit side, one expects the elastic wall to deform and tilt relative to the average substrate surface plane, see fig. 9. Here we show how one can include the fluid pressure when calculating the leak rate of seals. For simplicity we focus on the simplest case where the fluid pressure only depends on one coordinate x , as would be the case for most seal applications, *e.g.*, rubber O-ring seals, see fig. 9. In this case, for a stationary situation (15) takes the form

$$\frac{d}{dx} \left(\sigma_{\text{eff}}(p_{\text{cont}}(x)) \frac{d}{dx} p_{\text{fluid}}(x) \right) = 0,$$

or

$$\sigma_{\text{eff}}(p_{\text{cont}}(x)) \frac{d}{dx} p_{\text{fluid}}(x) = B,$$

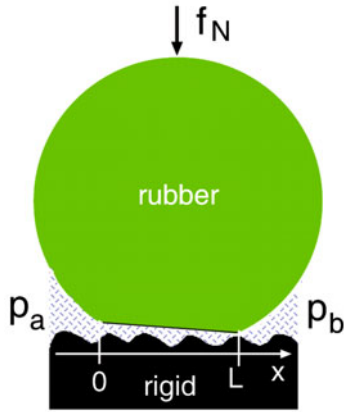


Fig. 9. Cross-section of rubber O-ring squeezed against a rigid, randomly rough surface in a fluid. The fluid pressure is higher at $x \approx 0$ than for $x \approx L$, *i.e.*, $p_a > p_b$, which results in fluid flow at the interface, from the left to the right. When p_a is comparable to the nominal squeezing pressure f_N/L (where f_N is the squeezing force per unit length of the cylinder), the elastic solid wall will deform and tilt as indicated in the figure.

where B is a constant. From this equation we get

$$p_{\text{fluid}}(x) = A + B \int_0^x dx' \sigma_{\text{eff}}^{-1}(p_{\text{cont}}(x')), \quad (25)$$

where A is a constant. If the fluid pressure for $x < 0$ (high-pressure side) is denoted by p_a , and for $x > L$ (low-pressure side) by p_b , then using that $p_{\text{fluid}}(0) = p_a$ and $p_{\text{fluid}}(L) = p_b$, we can determine the constants A and B in (25) and get $A = p_a$ and

$$B = \frac{p_b - p_a}{\int_0^L dx' \sigma_{\text{eff}}^{-1}(p_{\text{cont}}(x'))}. \quad (26)$$

Substituting these results in (25) gives

$$p_{\text{fluid}}(x) = p_a + (p_b - p_a) \frac{\int_0^x dx' \sigma_{\text{eff}}^{-1}(p_{\text{cont}}(x'))}{\int_0^L dx' \sigma_{\text{eff}}^{-1}(p_{\text{cont}}(x'))}. \quad (27)$$

The rubber O-ring is squeezed against the substrate by the normal force per unit radial length, f_N , see fig. 9. In the contact region between the cylinder and the substrate occur a nominal (locally averaged) pressure:

$$p_0(x) = p_{\text{cont}}(x) + p_{\text{fluid}}(x). \quad (28)$$

We consider a stationary case so that

$$\int_{-\infty}^{\infty} dx p_0(x) = \frac{f_N}{L}. \quad (29)$$

The elastic deformation field [4]

$$\bar{u}(x) = u_c + \frac{x^2}{2R} - \frac{2}{\pi E^*} \int_{-\infty}^{\infty} dx' p_0(x') \log \left| \frac{x - x'}{x'} \right|. \quad (30)$$

Equations (27), (28) and (30), together with the equation determining the relation between p_{cont} and \bar{u} , represent 4

equations for the 4 unknown variables p_0 , p_{cont} , p_{fluid} and \bar{u} . In addition, the pressure $p_0(x)$ must satisfy the normalization condition (29) which determines the parameter u_c in (30).

The leak rate of the seal is given by $\dot{Q} = J_x L_y$, where L_y is the width of the seal (*e.g.*, the circumference of the seal for a rubber O-ring). Using (13), we get

$$\dot{Q} = -L_y \sigma_{\text{eff}}(p_{\text{cont}}(x)) \frac{d}{dx} p_{\text{fluid}}(x) = -L_y B.$$

Using (26), this gives

$$\dot{Q} = \frac{L_y (p_a - p_b)}{\int_0^L dx' \sigma_{\text{eff}}^{-1}(p_{\text{cont}}(x'))}. \quad (31)$$

If p_{cont} is constant, this gives

$$\dot{Q} = \frac{L_y}{L_x} \sigma_{\text{eff}}(p_a - p_b), \quad (32)$$

where we now denote $L = L_x$. Equation (32) agrees with the result presented in ref. [11].

For elastically soft materials like rubber the calculation of the leak rate presented above can be simplified because a small change in the interfacial separation will have a negligible influence on the (locally averaged) stress distribution in the nominal contact area. Thus we can consider $p_0(x)$ as a given fixed function obtained by squeezing the elastic solid against a flat surface in the absence of the fluid. Using (27) and (28), we get

$$p_{\text{cont}}(x) = p_0(x) - p_a + (p_a - p_b) \frac{\int_0^x dx' \sigma_{\text{eff}}^{-1}(p_{\text{cont}}(x'))}{\int_0^L dx' \sigma_{\text{eff}}^{-1}(p_{\text{cont}}(x'))}. \quad (33)$$

This equation can be iterated to obtain the solution $p_{\text{cont}}(x)$. If the interfacial separation $\bar{u} > 2h_{\text{rms}}$, we can obtain the interfacial separation \bar{u} from p_{cont} using

$$\bar{u} = u_0 \log(\beta E^* / p_{\text{cont}}),$$

but in general the relation between \bar{u} and p_{cont} must be calculated from (A.4).

6 Experimental

We have performed a very simple experiment to test the theory presented in sect. 5. In fig. 10 we show our set-up for measuring the leak rate of seals. A glass (or PMMA) cylinder with a rubber ring (with rectangular cross-section) attached to one end is squeezed against a hard substrate with well-defined surface roughness. The cylinder is filled with water, and the leak rate of the fluid at the rubber countersurface is detected by the change in the height of the fluid in the cylinder. In this case the pressure difference $\Delta p = p_a - p_b = \rho g H$, where g is the gravitation constant, ρ the fluid density and H the height of the fluid column. With $H \approx 1$ m, we get typically $\Delta p \approx 0.01$ MPa. In the present study we

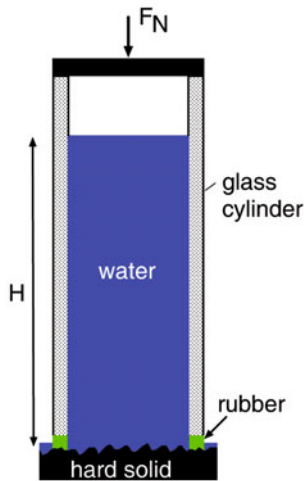


Fig. 10. Experimental set-up for measuring the leak rate of seals. A glass (or PMMA) cylinder with a rubber ring attached to one end is squeezed against a hard substrate with well-defined surface roughness. The cylinder is filled with water, and the leak rate of water at the interface between the rubber and the countersurface is detected by the change in the height of the water in the cylinder.

use a rubber ring with Young's elastic modulus $E = 2.3$ MPa, and with the inner and outer diameter 4 cm and 6 cm, respectively, and the height 0.5 cm. The rubber ring was made from a silicon elastomer (PDMS) prepared using a two-component kit (Sylgard 184) purchased from Dow Corning (Midland, MI). The kit consists of a base (vinyl-terminated polydimethylsiloxane) and a curing agent (methylhydrosiloxane-dimethylsiloxane copolymer) with a suitable catalyst. From these two components we prepared a mixture 10:1 (base/cross-linker) in weight. The mixture was degassed to remove the trapped air induced by stirring from the mixing process and then poured into casts. The bottom of these casts was made from glass to obtain smooth surfaces. The samples were cured in an oven at 80°C for 12 h.

We have used a sand-blasted PMMA as substrate. The root-mean-square roughness of the surface is $34\ \mu\text{m}$. In ref. [11] we show the height probability distribution $P(h)$ and the power spectrum $C(q)$ of the PMMA surface.

7 Experimental results and comparison with theory

In earlier studies we have performed experiments with the external load so large that the condition $p_0 \gg \Delta p$ was satisfied, which is necessary in order to be able to neglect the influence on the contact mechanics from the fluid pressure at the rubber countersurface [11, 21]. However, here we are interested in the situation where the fluid pressure is comparable to the nominal squeezing pressure. We use the normal load 18.5 N giving the nominal squeezing pressure $p_0 = 11.8$ kPa. Using a water column with height $H = 1.2$ m gives the fluid pressure $p_a - p_b = 11.8$ kPa

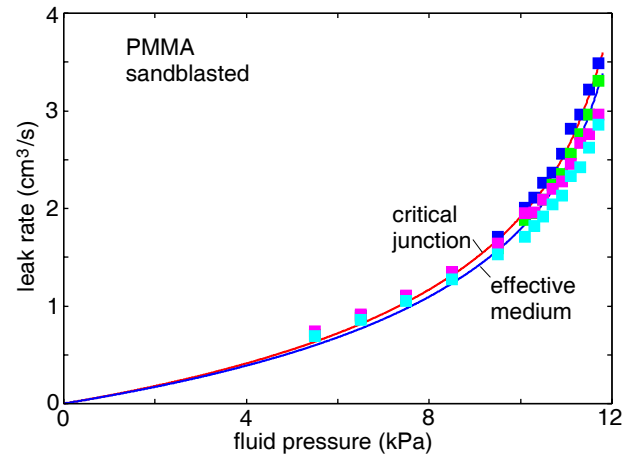


Fig. 11. Fluid leak rate as a function of the fluid pressure difference $\Delta p = p_a - p_b$. The nominal squeezing pressure is $p_0 = 11.8$ kPa. The square symbols are measured data while the solid lines are the theory predictions. In the calculation we used $\alpha' = 0.54$. For sandblasted PMMA with root-mean-square roughness $34\ \mu\text{m}$.

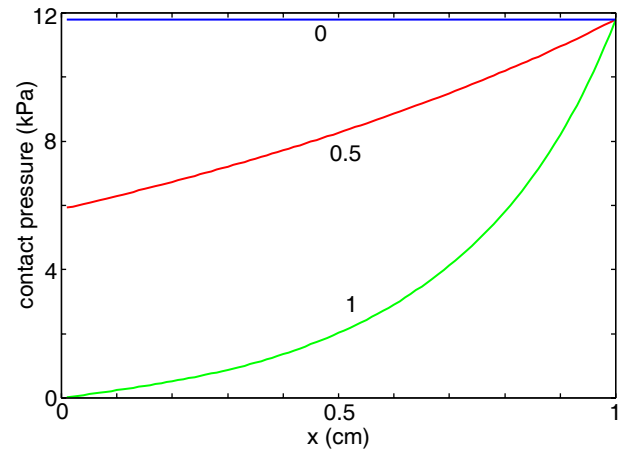


Fig. 12. The contact pressure as a function of the distance x between the high-pressure and low-pressure side. The nominal squeezing pressure is 11.8 kPa. Calculations are shown for $(p_a - p_b)/p_0 = 0, 0.5$ and 1. For sandblasted PMMA with root-mean-square roughness $34\ \mu\text{m}$.

at the bottom of the fluid column, which is equal to the squeezing pressure.

Let us compare the theory to experiment. In fig. 11 we show the fluid leak rate as a function of the fluid pressure difference $\Delta p = p_a - p_b$. The square symbols are measured data while the solid lines are the theory predictions. Note that the fluid leak rate rapidly increases when the fluid pressure Δp approaches the nominal squeezing pressure $p_0 = 11.8$ kPa. Note also that both the critical junction and the effective medium theories predict nearly the same pressure dependence of the leak rate as observed in the experiment.

In fig. 12 we show the calculated contact pressure as a function of the distance x between the high-pressure and low-pressure side. Calculations are shown for

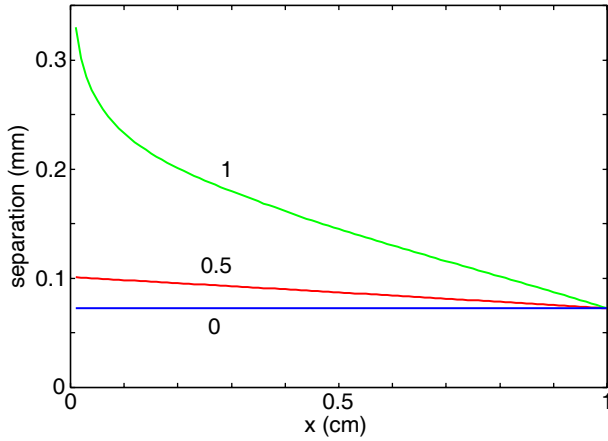


Fig. 13. The interfacial separation as a function of the distance x between the high-pressure and low-pressure side. The nominal squeezing pressure is $p_0 = 11.8$ kPa. Calculations are shown for $(p_a - p_b)/p_0 = 0, 0.5$ and 1 . For sandblasted PMMA with root-mean-square roughness $34 \mu\text{m}$.

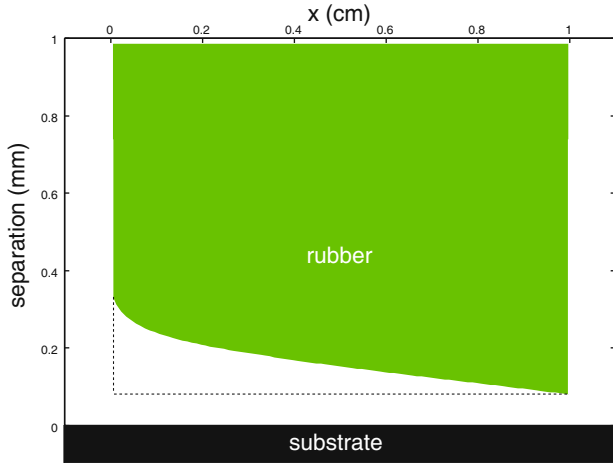


Fig. 14. Shape of the rubber block for $p_a - p_b = p_0$. The nominal squeezing pressure is $p_0 = 11.8$ kPa. The dashed line is the shape of the block when $p_a - p_b = 0$. For sandblasted PMMA with root-mean-square roughness $34 \mu\text{m}$.

$(p_a - p_b)/p_0 = 0, 0.5$ and 1 . In fig. 13 we show the interfacial separation as a function of the distance x between the high-pressure and low-pressure side. In fig. 14 we show for $p_a - p_b = p_0$ the deformed rubber block. The dashed line indicates the rubber block when $p_a - p_b = 0$. In this case the average separation is determined by the substrate surface roughness.

8 Summary and conclusion

In this paper we have studied fluid squeeze-out from the interface between an elastic solid with a flat surface and a randomly rough surface of a rigid solid. We have presented a general formalism for calculating the (average) interfacial separation as a function of time. In the theory enters the effective flow conductivity σ_{eff} . This quantity is a function of the (local) contact pressure p_{cont} .

In this paper we have calculated σ_{eff} using the so-called average-separation and critical-junction theories. An even more accurate method, based on the Bruggeman effective-medium theory, was developed in ref. [11], but this theory gives results very similar to the critical-junction theory. The critical-junction theory and the effective-medium theory both consider the flow of fluid in interfacial channels and the possibility (at high enough squeezing pressures) of trapped fluid at the interface as a result of percolation of the contact area, resulting in confined regions (islands) of non-contact area filled with fluid. We have shown how this affects the time dependence of the interfacial separation. We have shown how the present theory can be used to calculate the leak rate of static seals when including the reduction in the contact pressure resulting from the fluid pressure acting on the solids in the interfacial region. We have presented new experimental data which agree very well with the theory prediction.

This work, as part of the European Science Foundation EUROCORES Program FANAS, was supported from funds by the DFG and the EC Sixth Framework Program, under contract N ERAS-CT-2003-980409.

Appendix A.

Consider the elastic contact between two solids with randomly rough surfaces. The (apparent) relative contact area $A(\zeta)/A_0$ at the magnification ζ can be obtained using the contact mechanics formalism developed elsewhere [10, 22–26], where the system is studied at different magnifications ζ . We have [10, 25]

$$\frac{A(\zeta)}{A_0} = \frac{1}{(\pi G)^{1/2}} \int_0^{P_0} d\sigma e^{-\sigma^2/4G} = \text{erf} \left(\frac{P_0}{2G^{1/2}} \right), \quad (\text{A.1})$$

where

$$G(\zeta) = \frac{\pi}{4} \left(\frac{E}{1-\nu^2} \right)^2 \int_{q_0}^{\zeta q_0} dq q^3 C(q), \quad (\text{A.2})$$

where $C(q)$ is the surface roughness power spectrum, and where E and ν are Young's elastic modulus and Poisson ratio of the rubber.

We define $u_1(\zeta)$ to be the (average) height separating the surfaces which appear to come into contact when the magnification decreases from ζ to $\zeta - \Delta\zeta$, where $\Delta\zeta$ is a small (infinitesimal) change in the magnification. $u_1(\zeta)$ is a monotonically decreasing function of ζ , and can be calculated from the average interfacial separation $\bar{u}(\zeta)$ and $A(\zeta)$ using (see ref. [24])

$$u_1(\zeta) = \bar{u}(\zeta) + \bar{u}'(\zeta) A(\zeta)/A'(\zeta). \quad (\text{A.3})$$

The quantity $\bar{u}(\zeta)$ is the average separation between the surfaces in the apparent contact regions observed at the

magnification ζ , and can be calculated from [24]

$$\bar{u}(\zeta) = \sqrt{\pi} \int_{\zeta q_0}^{q_1} dq q^2 C(q) w(q, \zeta) \times \int_{p(\zeta)}^{\infty} dp' \frac{1}{p'} e^{-[w(q, \zeta) p' / E^*]^2}, \quad (\text{A.4})$$

where $p(\zeta) = p_0 A_0 / A(\zeta)$ (where $p_0 = p_{\text{cont}}$ denotes the nominal contact pressure) and

$$w(q, \zeta) = \left(\pi \int_{\zeta q_0}^q dq' q'^3 C(q') \right)^{-1/2}.$$

We will now show that as $p_0 \rightarrow 0$, for the values of the magnification ζ which are most important for the fluid flow between the solids, $u_1(\zeta) \rightarrow \bar{u}(\zeta)$. This result is physically plausible because at low contact pressures the separation between the walls is large and the surface roughness should have a very small influence on the fluid flow, which therefore can be accurately studied using the (average) interfacial separation \bar{u} for $\zeta \approx 1$.

Most of the fluid flow occurs in the flow channels which appear close to the percolation limit where $A(\zeta)/A_0 \approx 0.5$, or, using (A.1), for $p_0/G^{1/2}(\zeta) \approx 1$. Thus as $p_0 \rightarrow 0$ we must have $G(\zeta) \rightarrow 0$ which, using (A.2), implies $\zeta \rightarrow 1$. In fact, using $G(\zeta) \sim p_0^2$ and (A.2), one can easily show that for ζ close to unity $\zeta - 1 \sim p_0^2$. From (A.4) it is easy to show that as $p_0 \rightarrow 0$, the average separation $\bar{u}(\zeta)$ will diverge as $\sim -\log p_0$, while $\bar{u}'(\zeta)$ diverge as $-p'(\zeta)/p(\zeta) = A'(\zeta)/A(\zeta)$. Thus the product $\bar{u}'(\zeta)A'(\zeta)/A(\zeta)$ remains constant as $p_0 \rightarrow 0$. It follows from (A.3) that as $p_0 \rightarrow 0$, $u_1(\zeta) \rightarrow \bar{u}(\zeta)$.

Note that from (A.1) and (A.2) one can calculate

$$\frac{A'(\zeta)}{A(\zeta)} \approx \frac{1}{4(\zeta - 1)} \sim p_0^{-2},$$

so the slope of the curve $A(\zeta)$ in the relevant ζ -region becomes very high as $p_0 \rightarrow 0$.

References

1. B.N.J. Persson, C. Yang, J. Phys.: Condens. Matter **20**, 315011 (2008).
2. B.N.J. Persson, J. Phys.: Condens. Matter **20**, 315007 (2008).
3. F.P. Bowden, D. Tabor, *Friction and Lubrication of Solids* (Wiley, New York, 1956).
4. K.L. Johnson, *Contact Mechanics*, (Cambridge University Press, Cambridge, 1966).
5. B.N.J. Persson, *Sliding Friction: Physical Principles and Applications*, 2nd edition (Springer, Heidelberg, 2000).
6. J.N. Israelachvili, *Intermolecular and Surface Forces* (Academic, London, 1995).
7. See, e.g., B.N.J. Persson, O. Albohr, U. Tartaglino, A.I. Volokitin, E. Tosatti, J. Phys.: Condens. Matter **17**, R1 (2005).
8. B.N.J. Persson, Phys. Rev. Lett. **99**, 125502 (2007).
9. B.N.J. Persson, Surf. Sci. Rep. **61**, 201 (2006).
10. B.N.J. Persson, J. Chem. Phys. **115**, 3840 (2001).
11. B. Lorenz, B.N.J. Persson, Eur. Phys. J. E **31**, 159 (2010).
12. N. Patir, H.S. Cheng, J. Tribol., Trans. ASME **100**, 12 (1978).
13. N. Patir, H.S. Cheng, J. Tribol., Trans. ASME **101**, 220 (1979).
14. B.N.J. Persson, J. Phys.: Condens. Matter **22**, 265004 (2010).
15. B.N.J. Persson, B. Lorenz, A.I. Volokitin, Eur. Phys. J. E **31**, 3 (2010).
16. Strictly speaking, within fluid continuum mechanics for wetting liquids complete fluid squeeze-out never occurs. We have defined the area of real contact A by assuming that it can be obtained from the contact pressure p_{cont} using the contact mechanics theory of dry contacts.
17. B.N.J. Persson, M. Scaraggi, J. Phys.: Condens. Matter **21**, 185002 (2009).
18. S. Yamada, Tribol. Lett. **13**, 167 (2002).
19. B.N.J. Persson, U. Tartaglino, O. Albohr, E. Tosatti, Nat. Mater. **3**, 882 (2004).
20. B.N.J. Persson, J. Phys.: Condens. Matter **19**, 376110 (2007).
21. B. Lorenz, B.N.J. Persson, EPL **86**, 44006 (2009).
22. B.N.J. Persson, Surf. Sci. Rep. **61**, 201 (2006).
23. B.N.J. Persson, F. Bucher, B. Chiaia, Phys. Rev. B **65**, 184106 (2002).
24. C. Yang, B.N.J. Persson, J. Phys.: Condens. Matter **20**, 215214 (2008).
25. B.N.J. Persson, Phys. Rev. Lett. **99**, 125502 (2007).
26. The contact mechanics model developed in refs. [10, 22–25, 27] takes into account the elastic coupling between the contact regions in the nominal rubber-substrate contact area. Asperity contact models, such as the “standard” contact mechanics model of Greenwood-Williamson [28], and the model of Bush *et al.* [29], neglect this elastic coupling, which results in highly incorrect results [30, 31], in particular for the relations between the squeezing pressure and the interfacial separation [32].
27. B.N.J. Persson, J. Phys.: Condens. Matter **20**, 312001 (2008).
28. J.A. Greenwood, J.B.P. Williamson, Proc. R. Soc. London, Ser. A **295**, 300 (1966).
29. A.W. Bush, R.D. Gibson, T.R. Thomas, Wear **35**, 87 (1975).
30. C. Campana, M.H. Müser, M.O. Robbins, J. Phys.: Condens. Matter **20**, 354013 (2008).
31. G. Carbone, F. Bottiglione, J. Mech. Phys. Solids **56**, 2555 (2008).
32. B. Lorenz, B.N.J. Persson, J. Phys.: Condens. Matter **201**, 015003 (2009).